Impact of Land Surface Temperature (LST) and Ground Air Temperature (T$_{air}$) on Land Use and Land Cover (LULC): An Investigative Study

Duda B. Balas [a*], Mukesh Kumar Tiwari [a], Mukesh Trivedi [b] and Gautam R. Patel [c]

[a] *Department of Soil and Water Conservation Engineering Department, College of Agricultural Engineering and Technology, AAU, Godhra, Gujarat, India.*
[b] *Polytechnic in Agricultural Engineering, AAU, Dahod, Gujarat, India.*
[c] *Department of Agricultural Engineering, College of Agriculture, Anand Agricultural University, Vaso, Gujarat, India.*

Authors' contributions

This work was carried out in collaboration among all authors. All authors read and approved the final manuscript.

Original Research Article

ABSTRACT

The Land Surface Temperature (LST) is the fundamental concept of measuring the temperature of the ground or soil using remote sensing technologies. LST is an essential environmental parameter that has several uses in meteorology, climatology, agriculture, urban planning, and environmental monitoring. Remote sensing instruments, such as thermal infrared sensors aboard satellites, provide the means to capture LST data on a global scale. LST and ground air temperature (T$_{air}$) are two related but distinct measures that provide valuable insights into different aspects: LST refers to the temperature of the Earth's surface, and it provides information about the temperature of the soil or crop canopy, which can impact plant growth and development, on the other hand T$_{air}$ measures

_____

Corresponding author: E-mail: balasdinesh2222 @gmail.com;

the temperature of the surrounding air, which influences the rate of evaporation, transpiration, and photosynthesis in plants. In this study, a linear regression equation was developed to correlate the LST and T_{air} using air temperature data of 19th March 2017, and 14th March 2021 from the two meteorological stations namely Veganpur and Main Maize Research Station (MMRS) of the Godhra region. The Landsat 8 thermal and optical bands were used to estimate LST, whereas Sentinel 2 optical data was used for the Land Use and Land Cover (LULC) purpose. To correlate LST with T_{air}, eight ground truth (GT) points were collected from both stations, namely the minimum and maximum air temperatures in 2017 and 2021. The satellite derived LST data and the maximum ground air temperature (T_{air_max}) were found to strongly concur, with an R^2 value of 0.97. It was noted that a temperature difference of 2.9°C was found between the maximum ground air temperature (T_{air_max}) and the Land Surface Temperature (LST). Study showed that from 2017 to 2021, the area used for agriculture, forestry, water bodies, and barren land decreased from 75.62 to 71.51%, 15.17 to 14.30%, 1.60 to 1.38%, and 0.03 to 0.02%, respectively, however the area used for build-up increased from 7.59 to 12.79%. During a five-year period, the study identified an enhancement in Land Surface Temperature (LST) due to an increase in built-up area. A temperature change was also seen throughout the course of the five-year period as a result of variations in LULC. Overall, it came to light that, under specific conditions and speculation, LST estimated using thermal data from Landsat 8 can be closely associated with ground air maximum temperature.

1. INTRODUCTION

Land Surface Temperature (LST) is a critical meteorological measure and plays an important role in climate change, evapotranspiration, urban climate, vegetation monitoring, and environmental studies and research [1-4]. The temperature that is experienced when the land surface is touched with the hands is known as the Land Surface Temperature (LST) or the skin temperature of the ground [5-9]. In short, the temperature emitted by the surface is called the Land Surface Temperature (LST) which is measured in degree Celsius (°C) or degree Kelvin (°K), or Fahrenheit (F).

LST is associated with various surface properties such as albedo, emissivity, and thermal properties of land use cover types. Each of these properties has a high degree of variability with the alteration in land use and land cover caused by rapid urban development. LST is influenced by a multitude of factors, including solar radiation, land cover type, soil properties, vegetation, and human activities [10,11]. Remote sensing technologies, particularly infrared sensors aboard satellites, have enabled the estimation of accurate LST data on a global scale. These sensors measure the thermal infrared radiation emitted by the Earth's surface, which is then translated into temperature values through sophisticated algorithms. Land Surface Temperature is a fundamental parameter in Earth science, playing a vital role in understanding the interactions between the land, atmosphere, and climate. Its applications are diverse and span various disciplines, making LST data a critical resource for addressing global environmental challenges.

The continuously increasing levels of greenhouse gases in the atmosphere have a significant impact on LST. The glaciers and ice sheets in the Arctic area melt due to a rise in LST, which causes flooding and sea level rise [6]. Rising temperatures will be accelerated in the future decades due to increased greenhouse gas emissions from the melting of permafrost soils [12,13]. The monsoon-dependent country's climate also gets affected by an increase in LST, which results in erratic and uneven rainfall that has a detrimental effect on Land Use Land Cover (LULC). Land Use Land Cover (LULC) is one of the most significant parameters for proper region identification [14]. The accelerated evolution of permeable surface to impermeable surface caused by LULC changes has a significant effect on both the local and regional environment [14]. Buildings, roads, industrial farms, and so on are examples of impermeable surfaces that can absorb shortwave incoming solar radiation while reducing outgoing longwave terrestrial emissions [15]. It is crucial to look into this phenomenon. As a result, several researchers have computed LST using different methods and techniques.

It was challenging to determine the LST of a specific region before the development of Earth Observation Satellites (EOS). It was often produced for a specific set of sample points and extrapolated into isotherms to convert point measurements into area measurements. Recent advancements in remote sensing satellites and high-resolution sensors enable the spatial estimation of LST [6,16]. LST is estimated by using thermal infrared (TIR) bands of satellites. Landsat 8 is an Earth observation satellite put into orbit by the United States on February 11, 2013. It ensures the persistent acquisition and availability of Landsat data with a two-sensor payload, the Operational Land Imager (OLI) and the Thermal Infrared Sensor (TIRS). These two instruments pile up data for nine shortwave and two longwave thermal bands (Department of the Interior U.S. Geological Survey, 2016).

Remote sensing enhances the ability to measure the LST for large areas without direct contact with the object [17,18]. In the last few decades many researches have conducted different studies on the thermal analysis utilizing data derived from MODIS, ASETR, Landsat TM/ETM, and Landsat 8 [19].

The present study was undertaken to estimate the remote sensing based LST and compare it to maximum air temperature (T_{air_max}), minimum air temperature (T_{air_min}) and average air temperature (T_{air_avg}) in the Godhra region. In this study, the remote sensing derived LST was estimated using the Landsat-8 (optical and thermal bands) data, and the results were compared with the in situ T_{air} database obtained from two agrometeorological stations located in the study area. The term LST refers to remote sensing-derived surface temperature, whereas T_{air} refers to air temperature measurement using meteorological stations. Instead of presenting a validation strategy, this research compares LST with T_{air} records. In situ data, based on measurements of the emissivity of the earth's surface made using a thermal infrared radiometer (TIR) or other analogous devices, are necessary for a validation strategy of LST [20]. This research compares two parameters in particular, each of which has a distinct physical meaning.

LST is the radiation properties of the earth's surface and influences the intensity of long-wave radiation emitted by it, which is recorded by satellite-based remote sensing platforms. The air temperature is recorded at 1.5-2 m height by the sensor's contact with the surrounding air. T_{air} and Land Surface Temperature (LST) are linked to each other to establish a relationship among them. A linear regression equation is used to compare the two parameters i.e., LST and T_{air} using a measure of statistics called the coefficient of determination (R^2).

The principal objectives of the study were to compute the Land Surface Emissivity (LSE) using the Normalized Difference Vegetation Index (NDVI) threshold approach, calculate the brightness temperature using band 10 of the TIR, and determine the LST of the Godhra tehsil, located in Middle Gujarat region, India, and to compare LST with the ground air temperature (T_{air}) using the Mono-Window (SW) algorithm.

2. MATERIALS AND METHODS

2.1 Study Area

The present study area comprised of Godhra *tehsil*, which comes under the Panchmahal district of Gujarat, India as shown in Fig. 1. The study region is located between latitudes 22°41'51"N to 22°53'35"N and longitudes 73°21'08"E to 73°51'11"E, with a total area of about 772 km^2 and an estimated population of 4,62,516 (census-2011). The average annual rainfall varies from 65 to 75 cm, while minimum and maximum temperature ranges from 6 ^{0}C (cold winter) and 44 ^{0}C (hot summer). The soil type of the study area is sandy and sandy loam. In the research region, there are typically four distinct seasons: winter (November – February), summer (March–May), monsoon (June – September), and autumn (October). Farmers in this region grow crops like maize, rice, millet, legumes, cotton, etc., with two to three crops per year. Furthermore, it is a rapidly growing tehsil in the Panchmahal district because a lot of new transmutation of land have been seen in the recent time period. Throughout the rainy season, the vegetation looks green and healthy, as a consequence of an increase in chlorophyll.

Two agrometeorological stations viz. Panam High Level Canal Subdivision No-4, Veganpur (here onward it is mentioned as Veganpur) and Main Maize Research Station (MMRS) located in the study region (Fig. 1) are considered in this study. Both stations are located 25 km apart. MMRS is nearest to the main city whereas, Veganpur is 20 km away from the main city.
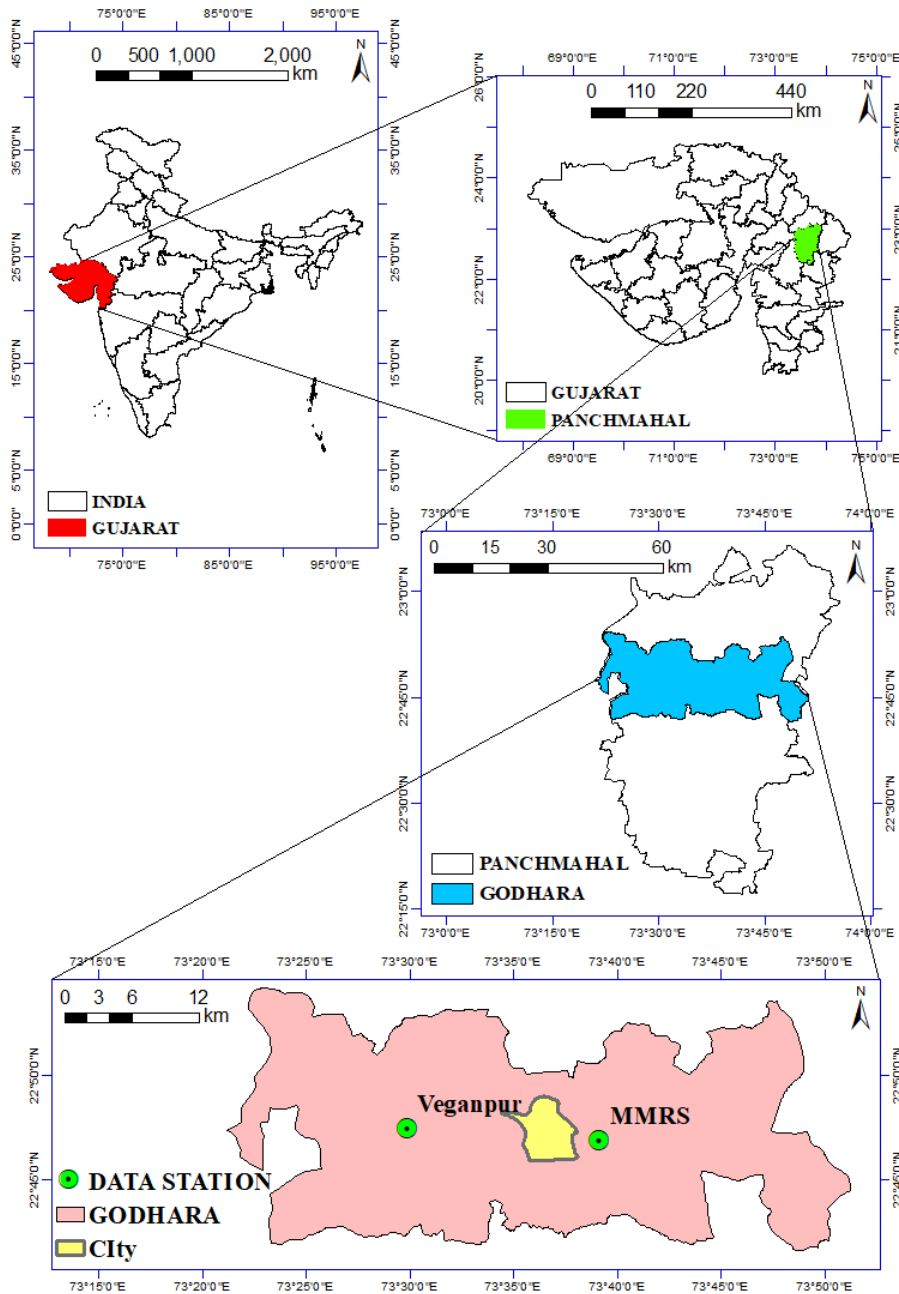
Fig. 1. Location map of the study area

2.2 Data Collection

The LANDSAT-8 OLI and TIRS images pertaining to the study area were downloaded from the USGS Earth Explorer data center website (https://earthexplorer.usgs.gov/). Specifications of the satellite and data used in this study are described in Table 1. Moreover, air temperature data such as maximum air temperature (T_{air_max}), and minimum air temperature (T_{air_min}) for two ground stations were collected from Veganpur (73°29'48.6"E, 22°47'36.742"N) and Main Maize Research Station (MMRS) (73°38'24.374"E, 22°47'5.588"N), located in the study area. A total of eight ground truth (GT) points were collected from both sites, namely the minimum and maximum temperatures in 2017 and 2021.

Table 1. Specifications of satellite data

Satellite/ Sensor	Specifications			
Landsat 8 OLI & TIRS	Acquisition date		19th March-2017 14th March-2021	
	Spatial Resolution		30 m (OLI) & 100 m (TIRS)	
	Path / Row		148 / 44	
	Data Product		Collection-1 and Level-1	
	Band	**Resolution, m**	**Wavelength, μm**	**Band information, m**
	1	30	0.43–0.45	Coastal aerosol
	2	30	0.45–0.51	Blue
	3	30	0.53–0.59	Green
	4	30	0.64–0.67	Red
	5	30	0.85–0.88	Near Infrared (NIR)
	6	30	1.57–1.65	SWIR-1
	7	30	2.11–2.29	SWIR-2
	8	15	0.50–0.68	Panchromatic
	9	30	1.36–1.38	Cirrus
	10	100	10.6–11.19	Thermal Infrared (TIRS)-1
	11	100	11.50–12.51	Thermal Infrared (TIRS)-2

2.3 Pre-processing Steps for Estimating Land Surface Temperature (LST)

The Landsat 8 Operational Land Imager (OLI) band 4 and band 5 data and Thermal Infrared Sensor (TIR) band 10 digital data were analyzed to estimate the Land Surface Temperature (LST) of the study area. In this research TIR band 10 is used for LST derivation instead of band 11 because TIR band 11 has larger uncertainties for LST derivation. The entire bit-by-bit procedure to enumerate LST described by Avdan and Jovanovska [8] was followed in this study as discussed below along with a flow chart showing the methodology in Fig. 2.

2.3.1 Top of atmospheric spectral radiance

$$L\lambda = M_l \times Q_{cal} + A_l - Q_i \qquad (1)$$

Where,

	$L\lambda$	=	Top of atmospheric spectral radiance $\left(\frac{watts}{m^2 \times ster \times \mu m}\right)$
	M_l	=	Radiance multiplicative rescaling factor
	A_l	=	Band-specific additive rescaling factor
	Q_{cal}	=	Quantized and calibrated standard product pixel values (DN)
	Q_i	=	Correction value for band 10

2.3.2 Conversion of radiance to at sensor temperature

$$BT = \left(\frac{K_2}{\ln\left(\frac{K_1}{L\lambda + 1}\right)}\right) - 273.15 \qquad (2)$$

Where,

	BT	=	Brightness temperature (°C)
	K_1	=	Band-specific thermal constants (Table 2)
	K_2	=	Band-specific thermal constants (Table 2)

Table 2. Landsat-8 metadata of the study area

Thermal	K_1	774.8853
Constant	K_2	1321.0789
Rescaling	M_l	0.00033
Factor	A_l	0.1

2.3.3 Normalized difference vegetation index (NDVI)

$$NDVI = \left(\frac{NIR - RED}{NIR + RED}\right) \qquad (3)$$

Where,

	NIR	=	DN value from Near Infrared (band 5)
	RED	=	DN value from Red (band 4)

2.3.4 Proportion of vegetation (P$_V$)

$$P_v = \left(\frac{NDVI - NDVI_{min}}{NDVI_{max} - NDVI_{min}}\right)^2 \qquad (4)$$

Where,

P_v	=	Proportion of vegetation
NDVI	=	Normalized Difference Vegetation Index
$NDVI_{max}$	=	Maximum value of Normalized Difference Vegetation Index
$NDVI_{min}$	=	Minimum value of Normalized Difference Vegetation Index

2.3.5 Land surface emissivity (LSE)

$$LSE = 0.004 \times P_v + 0.986 \qquad (5)$$

2.3.6 Land surface temperature (LST)

$$LST = \frac{BT}{\left(1 + \left(\frac{\lambda \times BT}{C_2}\right)\right) \times \ln E} \qquad (6)$$

Where,

λ	=	Limiting wavelength 10.895 for band 10

C_2	=	$\left(\frac{h \times c}{s}\right) = 14388$
h	=	Plank's constant = 6.626×10^{-34} J-s
c	=	Velocity of light = 2.998×10^8 m/s
s	=	Boltmanz constant = 1.38×10^{-23} J-K

2.4 Land Use Land Cover

LULC thematic map was downloaded from https://www.arcgis.com/home/item.html?id=fc92d38533d440078f17678ebc20e8e2 provided by ESRI, Microsoft, and Impact Observatory which was prepared from Sentinal-2 data. Sentinel-2 satellite has a spatial resolution of 10 m, which was helpful in identifying and analysing land cover and localities in 2017 and 2021. Furthermore, a ground survey of the study area was conducted to validate the LULC data with satellite images.
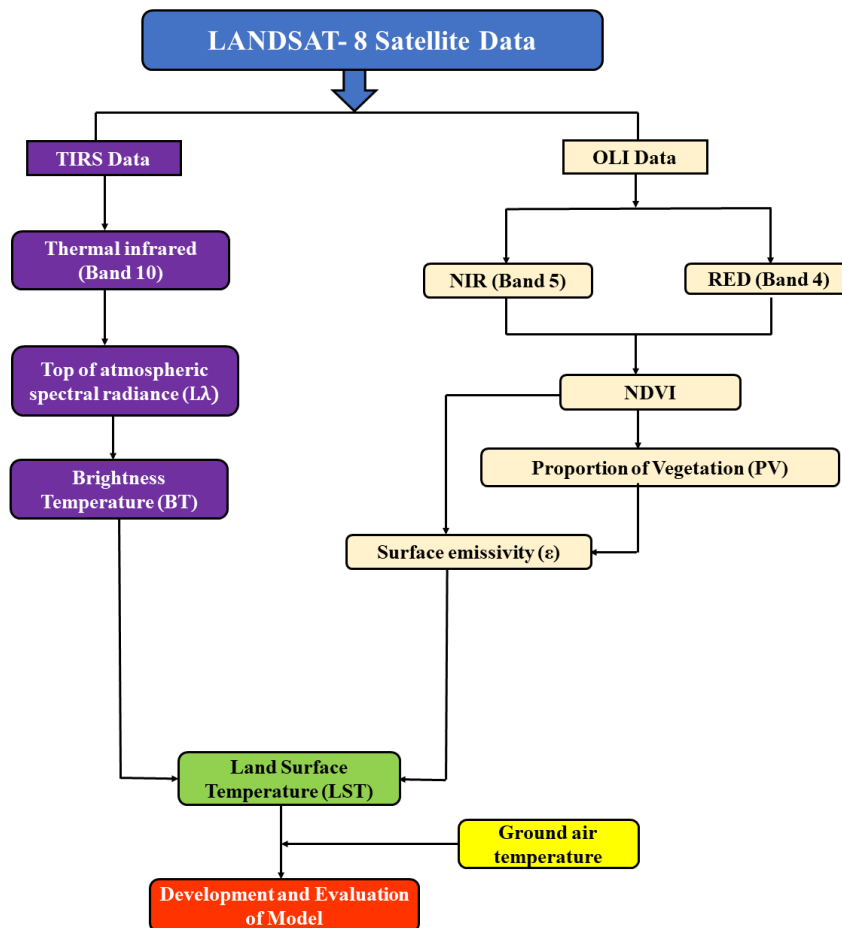

Fig. 2. A flowchart of the process and data analysis

During the field investigation, major LULC classes such as agriculture, forest, water body, build-up, and barren land were identified. Different associated parameters like areas covered (km^2), the net change in the area (km^2), change in the area (%) and annual change rate (%) is calculated. The annual change rate (%) is calculated by following formula [21].

$$\text{Annual change rate}, \% = \left(\sqrt[j-i]{\frac{A_j}{A_i}} - 1 \right) \times 100 \qquad (7)$$

A$_j$ Areas of each land-cover category at time points j

A$_i$ Areas of each land-cover category at time points i

2.5 Model Evaluation

The coefficient of determination (R^2), which ranges from 0 to 1 was used to quantify how well a statistical model predicts a result as given by eq. (8):

$$R^2 = \left(\frac{\sum_{i=1}^{n}(O_i - \overline{O})(P_i - \overline{P})}{\sqrt{\sum_{i=1}^{n}(O_i - \overline{O})^2} \sqrt{\sum_{i=1}^{n}(P_i - \overline{P})^2}} \right)^2 \qquad (8)$$

Where,

O$_i$ Ground air temperature, °C

$\overline{O}$ Land Surface Temperature (LST), °C

3. RESULTS AND DISCUSSION

3.1 Change in Land Use Land Cover (LULC) from 2017 to 2021

LULC provided by Sentinal-2 was used in this study for both the years 2017 and 2021 because of high spatial resolution as shown in Figs. 4 & 5. In both years, agricultural land predominated, followed by forest, build-up, water bodies, and barren land revealed by the data given in Table 3. Except for the main rural city of Godhra, the remaining area is urbanized and mainly associated with farming and livestock [22].

The geography of the study area is undulating, with paved surfaces on the eastern-northern (EN) and eastern-southern (ES) sides. Additionally, there are mountainous and hilly areas with a significant presence of rocks, as depicted in Fig. 3 through the Digital Elevation Model (DEM). These topographical features contribute to the region experiencing higher surface temperatures, leading to the highest Land Surface Temperature (LST) values in this area. The combination of rugged terrain, paved surfaces, and rocky terrain can create conditions that lead to increase in LST, making it one of the hottest areas within the study area.

From 2017 to 2021, the area under agriculture, forest, water bodies, and barren land declined from 75.62 to 71.51 %, 15.17 to 14.30 %, 1.60 to 1.38 %, and 0.03 to 0.02 % respectively while the build-up area expanded from 7.59 to 12.79 % as shown in Figs. 4 & 5 and Table 3. Changes in agriculture, forest, water bodies, build-up, and barren land were observed to be -4.11 %, -0.87 %, -0.21 %, 5.20 %, and 0.00 %, respectively from 2017 to 2021. Overall, negative change was observed in agriculture, forests, and water bodies, while positive change was observed in build-up areas. The annual LULC change rate for build-up, agriculture, forest, water bodies, and barren land was remarked at 8.03, -6.35, -1.35, -0.33, and -0.01 percent, respectively as shown in (Table 3).

There was an abrupt change observed in the built-up and agricultural areas. Enhanced build-up area is due to industrialization, building construction, road construction, and migration of people from rural to urban areas, which leads to the construction of new houses for their sheltering. Several shopping centers, malls, civilizations, roadways, and industries have sprouted up in the last two years. Diminish in agricultural areas is because people are less likely to be interested in farming because of fragmentation of land, low income, and soil that is primarily suitable for low-value crops such as maize, rice, wheat, and sorghum. An increase in pedigree leads to population growth, whereas land remains constant; migration of people from rural to urban areas for survival, desire for a prosperous life and they also require a residence [23].

3.2 Validation of LST with Ground Air Temperature

Temperature data of 19th March 2017 and 14th March 2021 were collected from two data stations (Veganpur and MMRS) to compare the Landsat-8 satellite LST data. A comparison of LST-derived data of Landsat 8 with both ground stations having maximum, minimum, and average temperature data during 2017 and 2021 is presented in Fig. 5.
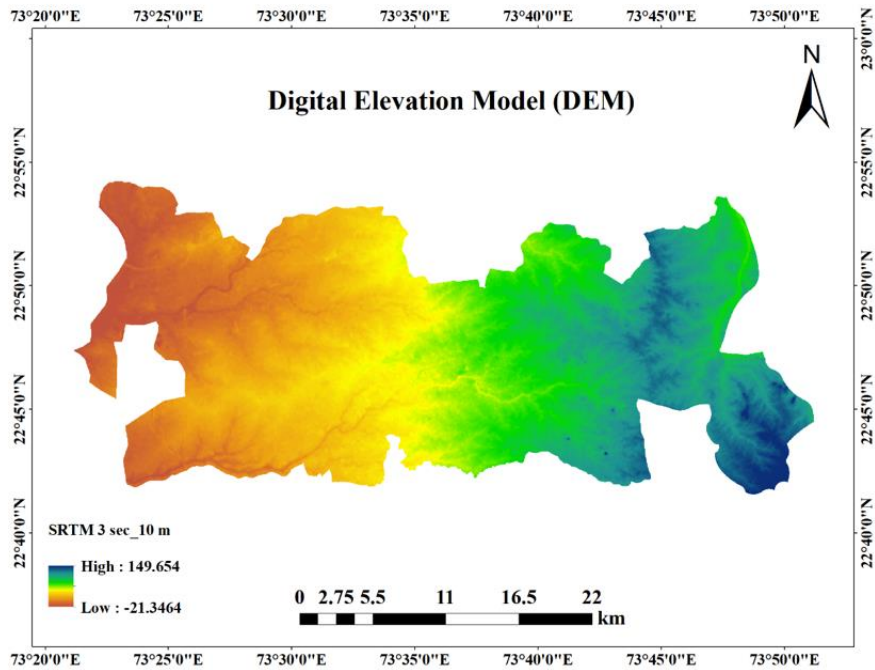
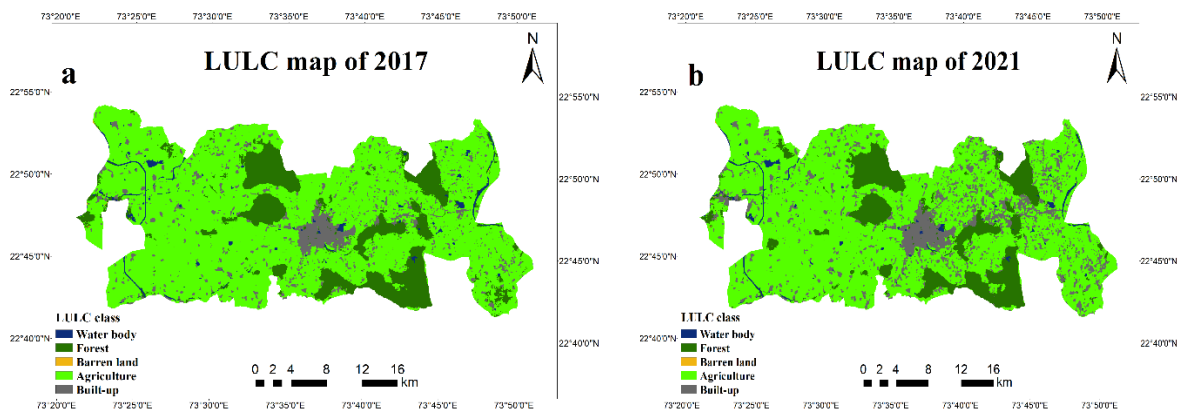**Fig. 3. Digital Elevation Model (DEM) of the study area**

Fig. 4. Land Use Land Cover (LULC) map of the study area for the year (a) 2017 and (b) 2021

Table 3. Area change and annual area change for various LULC classes in 2017 and 2021

Classes	2017		2021		Change in area, km²	Change in area, %	Annual change of area, km²
	Area, km²	Area, %	Area, km²	Area, %			
Agriculture	583.87	75.62	552.14	71.51	-31.73	-4.11	-6.35
Forest	117.12	15.17	110.37	14.30	-6.75	-0.87	-1.35
Build-up	58.58	7.59	98.74	12.79	40.17	5.20	8.03
Water body	12.32	1.60	10.67	1.38	-1.65	-0.21	-0.33
Barren land	0.20	0.03	0.16	0.02	-0.04	0.00	-0.01
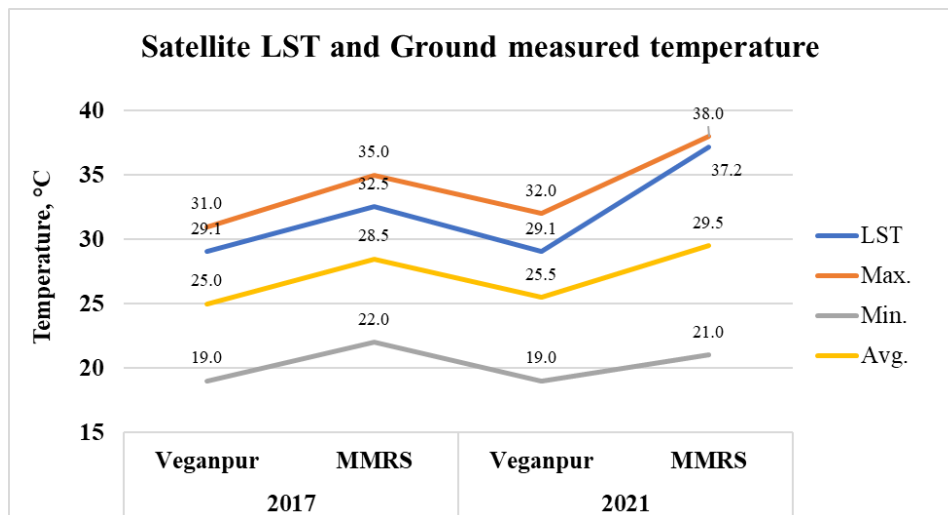
Fig. 5. LST and ground air temperature (T$_{air}$) data of the agrometeorological stations in 2017 and 2021

The least variation of LST was found with maximum ground temperature while minimum and average ground temperature data shows substantial variations with LST at both stations in 2017 and 2021. Satellite LST and maximum ground temperature difference were found 1.9 °C and 2.5 °C at Veganpur and MMRS station respectively in 2017. In the case of 2021, it was found 2.9 °C and 0.8 °C at Veganpur and MMRS stations respectively. Srivastava et al., (2010) compared ground air temperature and land surface temperature and reported a discrepancy of 5°C. The difference in LST and ground temperature is due to the resolution of LANDSAT 8 for the used bands is 100 m for the thermal band and 30 m for the red and NIR bands. Here, it is notable that the area surrounding Veganpur station is wet and almost irrigated whereas, the area surrounding MMRS station is almost dry, built up, rocky, and not irrigated during the summer season so, there is a big difference found in temperature data between both the stations and both are apart at 25 km.

It was observed that satellite-derived LST data has reasonably good agreement with maximum ground temperature having an R^2 value is 0.97 whereas, it was declined with minimum and average ground temperature having R^2 values are 0.50 and 0.89, respectively as seen in Figs. 6 to 8. In further analysis, we used maximum air temperature data because it shows a higher correlation to LST.
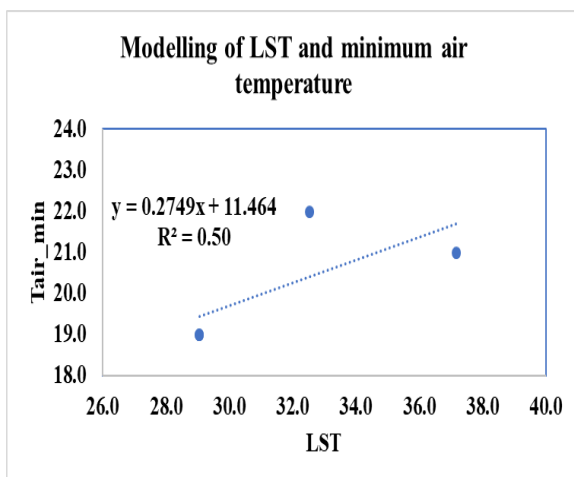

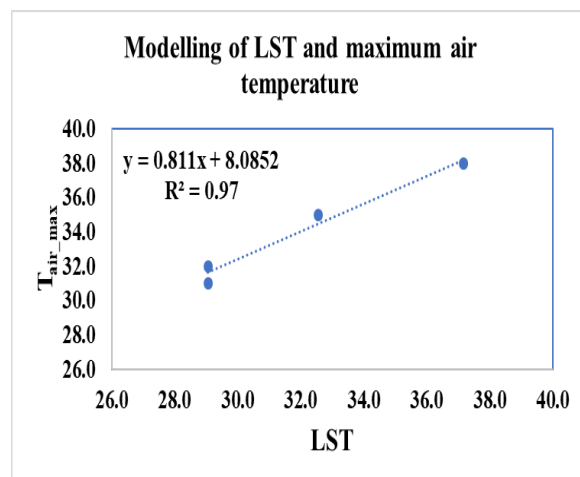**Fig. 6. Correlation of LST with minimum air temperature**

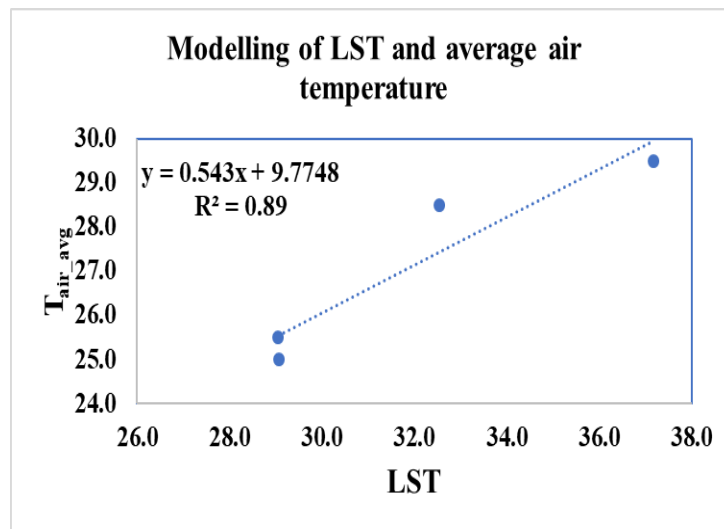**Fig. 7. Correlation of LST with maximum air temperature**

Fig. 8. Correlation of LST with average air temperature

Every year rise in temperature was found 0.005 ^{0}C and 0.93 ^{0}C at Veganpur and MMRS. It is stated that the rate of rise in temperature is higher at MMRS because it is closest to the main urban city, surrounded by built-up area, drastically decreased in trees and shrubs area, and irrigation is not provided to farms during the month of March, whereas Veganpur station is substantially surrounded by agriculture land, shrubs, and farms are irrigated, which can raise the humidity in the air results in lower air temperature.

3.3 LST Spatiotemporal Pattern

The LST ranged from 22.03 to 37.98 °C with an average value of 31.92 °C in 2017 whereas, 23.31 to 40.92 °C with an average value of 33.36 °C in 2021 as shown in Figs. 9 & 10. The

standard deviation of LST was 2.49 and 2.64 in 2017 and 2021, respectively. It was observed that LST has increased by 1.44 °C (average of 2021- average of 2017) over the last five years. The increase in LST is due to a drastic change in LULC as a direct consequence of a 5.20 % increase in build-up area, which results in an impervious surface over the land surface. An impervious surface absorbs sunlight and re-emits it in the form of heat. As stated in Table 3, the decline in forest area (-0.87), water body area (-0.21), and agriculture area (-4.11) emphasized to boost the LST. Furthermore, the Emission of vehicle smoke enhances the GHGs which leads to an increase in temperature and ultimately emphasizes on the LST acceleration. The environment is being harmed by a steadily increasing population that is building new houses and buying new vehicles to live a prosperous life.
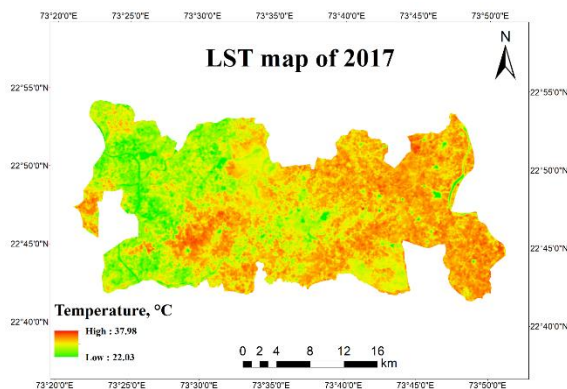

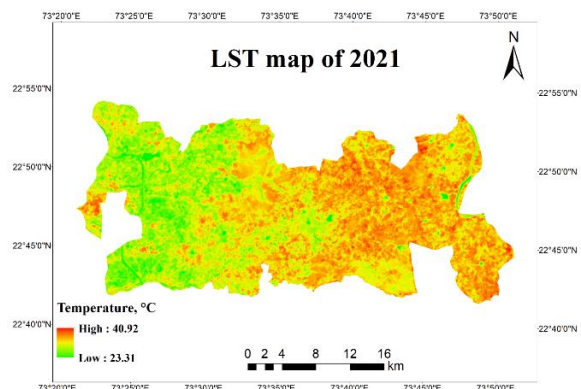**Fig. 9. Land Surface Temperature (LST) map of 19ᵗʰ March 2017**

Fig. 10. Land Surface Temperature (LST) map of 14 March 2021

3.4 Area Confined by Different LST Classes

The visual interpretation of different LST classes i.e., 23-26°C, 27-30°C, 31-34°C, 35-38°C, and 39-41°C are presented in Figs. 11 & 12. From both year figures it is clear that the area covered by 35-38°C has increased whereas, the area covered by 31-34°C, 27-30°C and 23-26°C declined in 2021 compared to 2017. The LST increased over the whole study region during five years, except few places where barren land was converted into agricultural land. The increase in LST was seen as a result of mining and deforestation caused by human intervention in the study area.

The Table 4 depicts the area covered by different LST classes (km^2), change in area (km^2), and annual change of area (km^2) from 2017 to 2021. From 2017 to 2021, the area covered by the 35-38 °C class rapidly changed and increased to 177.45 .45 km^2 (22.98%). Furthermore, a sharp fall of -108.47 km^2 (-14.05) was seen in the area covered by the 31-34 °C class over five years.

Over five years, two classes i.e., 35-38°C and 39-41°C saw an increase in the LST area, whereas the remaining classes i.e., 22°C, 23-26°C, 27-30°C, and 31-34°C saw a decrease. An annual change of area for the classes of 23-26°C, 27-30°C, 31-34°C, and 35-38°C were observed -1.78 km^2, -13.77 km^2, -21.69 km^2, and 35.49 km^2, respectively.

3.5 Ground Air Temperature

The simulation of LST with ground air temperature was carried out, and a map of the spatial variations of ground air temperature was generated, as shown in Figs. 13 & 14. The ground air temperature varies from 25.95 to 38.89°C with an average value of 34°C in 2017 and 26.99 to 41.27°C with an average of 35.17°C in 2021. The standard deviation of the ground air temperature was found 2.02 and 2.15 for 2017 and 2021, respectively. It was observed that ground air temperature has increased by 1.17°C (average of 2021- average of 2017) over the last five years.
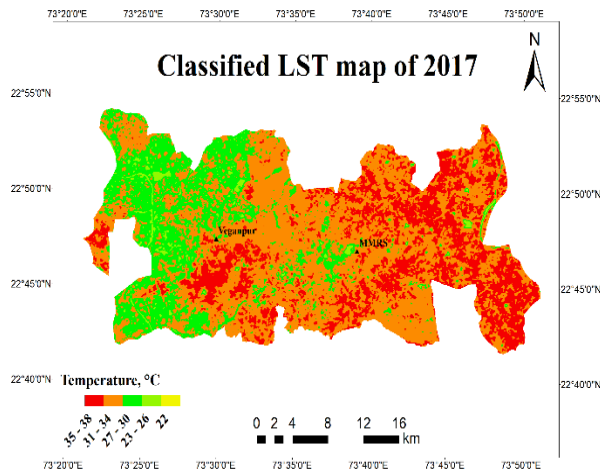

Fig. 11. Different Land Surface Temperature (LST) classes map of 19th March 2017
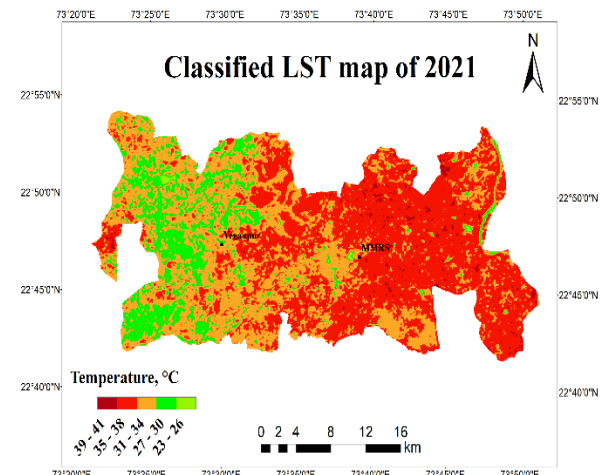

Fig. 12. Different Land Surface Temperature (LST) classes map of 14th March 2021

Table 4. Area change and annual area change for various LST classes from 2017 to 2021

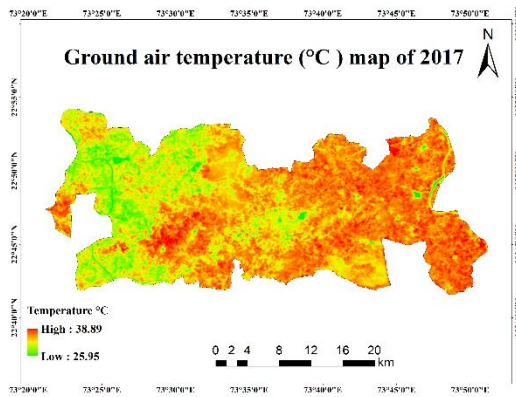| Classes	2017		2021		Change in area, km^2	Change in area, %	Annual change of area, km^2
	Area, km^2	Area, %	Area, km^2	Area, %			
39-41	-	-	8.79	1.14	-	-	-
35-38	180.22	23.34	357.67	46.32	177.45	22.98	35.49
31-34	416.91	54.00	308.44	39.95	-108.47	-14.05	-21.69
27-30	163.75	21.21	94.88	12.29	-68.87	-8.92	-13.77
23-26	11.22	1.45	2.33	0.30	-8.90	-1.15	-1.78
22	0.001	0.0001	-	-	-	-	-

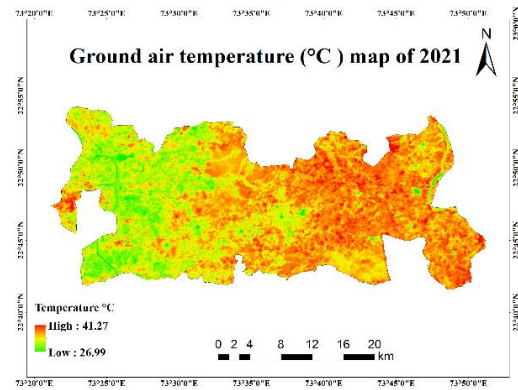**Fig. 13. Ground air temperature map of the study area in 2017**

Fig. 14. Ground air temperature map of the study area in 2021

4. CONCLUSION

The study was undertaken to simulate the Land Surface Temperature (LST) with ground air maximum (T_{air_max}), minimum (T_{air_min}) and average temperature (T_{air_avg}) using two meteorological stations (Veganpur and MMRS) data in Godhra region. Landsat 8 data were used to determine the Land Surface Temperature (LST), while Sentinel 2 data were used to for the purpose of Land Use and Land Cover (LULC). Moreover, temperature change as a consequence of the change in Land Use Land Cover (LULC) was also observed over the five-year period. To examine the annual difference and over five-year change in LST, ground air temperature, and LULC, the years 2017 and 2021 were chosen. From 2017 to 2021, it was found that changes in area of agriculture, forests, water bodies, build-up, and barren land were -4.11%, -0.87%, -0.21%, 5.20%, and 0.00%, respectively. In general, negative change was seen in area of agriculture, forests, and water bodies, whereas positive change was appeared in area of built-up. Maximum ground temperature (T_{air_max}) was found to have the least variance of LST, however minimum and average ground temperature data reveal significant differences with LST at both sites in 2017 and 2021. The difference between the maximum ground air temperature (T_{air_max}) and LST was assessed to be 2.9 °C. The maximum ground air temperature (T_{air_max}) and satellite-derived LST data were found to reasonably accord, with an R^2 value of 0.97. In 2017, the LST was varies from 22.03 to 37.98 °C, whereas in 2021, it varies from 23.31 to 40.92 °C. From 2017 to 2021, the LST has risen by 1.44 °C in the study area. Deforestation, mining on grazing land, growth of the built-up region, and diminished size of water bodies and agricultural land all contributed to an increase in the LST. Landsat 8 satellite derived LST can be simulated with maximum ground air temperature (T_{air_max}). Overall, this study discovered that by integrating Landsat 8 thermal data, the spatial ground air temperature distribution could be determined using the Land Surface Temperature (LST) estimation approach.

ACKNOWLEDGEMENT

COMPETING INTERESTS

Authors have declared that no competing interests exist.

REFERENCES

1. Anderson MC, Norman JM, Mecikalski JR, Otkin JA, Kustas WP. A climatological study of evapotranspiration and moisture stress across the continental United States based on thermal remote sensing: 1. Model Formulation. Journal of Geophysical Research: Atmospheres. 2007;112(D10).
2. Gallo K, Hale R, Tarpley D, Yu Y. Evaluation of the relationship between air and land surface temperature under clear- and cloudy-sky conditions. Journal of

Applied Meteorology and Climatology. 2011;50(3):767-775.

3. Balas D, Thakor D. Development of rainfall simulator to observe the real field runoff on sweet orange (Citrus X sinensis) orchard. The Pharma Innovation Journal. 2021; 10(11):1312-1317.

4. Ram B, Gaur ML, Patel G, Kunapara A, Pampaniya N, Damor P, Balas D. Assessment of Diurnal Variability and Region-Specific Connection across Intensity, Depth & Duration of Rainfall. International Journal of Environment and Climate Change. 2023;13(9):595-606.

5. Urban M, Eberle J, Hüttich C, Schmullius C, Herold M. Comparison of satellite-derived land surface temperature and air temperature from meteorological stations on the pan-Arctic Scale. Remote Sensing. 2013;5(5):2348-2367.

6. Rajeshwari A, Mani ND. Estimation of land surface temperature of Dindigul district using Landsat 8 data. International Journal of Research in Engineering and Technology. 2014;3(5):122-126.

7. Chinchorkar SS, Sayyad FG, Vaidya VB, Pandey V. Trend detection in annual maximum temperature and precipitation using the Mann Kendall test–A case study to assess climate change on Anand of central Gujarat. Mausam. 2015;66(1): 1-6.

8. Avdan U, Jovanovska G. Algorithm for automated mapping of land surface temperature using LANDSAT 8 satellite data. Journal of Sensors. 2016;1-8.

9. Sutariya S, Ankur H, Tiwari M. Development of modeler for automated mapping of land surface temperature using GIS and LANDSAT-8 Satellite Imagery. International Journal of Environment and Geoinformatics. 2022;9(2):54-59.

10. Dang H, Gillett NP, Weaver AJ, Zwiers FW. Climate change detection over different land surface vegetation classes. International Journal of Climatology: A Journal of the Royal Meteorological Society. 2007;27(2):211-220.

11. Mihailovic DT, Eitzinger J. Modelling temperatures of crop environment. Ecological Modelling. 2007;202(3-4):465-475.

12. Moritz RE, Bitz CM, Steig EJ. Dynamics of recent climate change in the Arctic. Science. 2002;297(5586):1497-1502.

13. Serreze MC, Walsh JE, Chapin FS, Osterkamp T, Dyurgerov M, Romanovsky V, Oechel WC, Morison J, Zhang T, Barry RG. Observational evidence of recent change in the northern high-latitude environment. Climatic Change. 2000; 46:159-207.

14. Rousta I, Sarif MO, Gupta RD, Olafsson H, Ranagalage M, Murayama Y, Zhang H, Mushore TD. Spatiotemporal analysis of land use/land cover and its effects on surface urban heat island using Landsat data: A case study of Metropolitan City Tehran (1988–2018). Sustainability. 2018; 10(12): 4433.

15. Ranagalage M, Estoque RC, Zhang X, Murayama Y. Spatial changes of urban heat island formation in the Colombo District, Sri Lanka: Implications for Sustainability Planning. Sustainability. 2018;10(5):1367.

16. Balas D, Tiwari M, Patel G. Estimation of surface and subsurface soil moisture using microwave remote sensing: A typical analysis. International Journal of Environment and Climate Change. 2023;13(10):1804–1816.

17. Guillevic P, Göttsche F, Nickeson J, Hulley G, Ghent D, Yu Y, Trigo I, Hook S, Sobrino JA, Remedios J, Camacho F. Land surface temperature product validation best practice protocol. Best practice for satellite-derived land product validation. 2018;60.

18. Celik B, Kaya S, Alganci U, Seker DZ. Assessment of the relationship between land use/cover changes and land surface temperatures: a case study of thermal remote sensing. Fresenius Environ. Bulletin. 2019;3:541.

19. Ibrahim M, Abu-Mallouh H. Estimate land surface temperature in relation to land use types and geological formations using spectral remote sensing data in Northeast Jordan. Open Journal of Geology. 2018;8(2):174-185.

20. Hachem S, Duguay CR, Allard M. Comparison of MODIS-derived land surface temperatures with ground surface and air temperature measurements in continuous permafrost terrain. The Cryosphere. 2012;6(1):51-69.

21. Dissanayake DMS LB, Morimoto T, Ranagalage M, Murayama Y. Land-use/land-cover changes and their impact on surface urban heat islands: Case study of Kandy City, Sri Lanka. Climate. 2019;7(8):99.

22. Srivastava PK, Han D, Ramirez MR, Islam T. Machine learning techniques for downscaling SMOS satellite soil moisture using MODIS land surface temperature for hydrological application. Water Resources Management. 2013;27:3127-3144.

23. Lv ZQ, Zhou QG. Utility of Landsat image in the study of land cover and land surface temperature change. Procedia Environmental Sciences. 2011;10:1287-1292.

Peer-review history:
The peer review history for this paper can be accessed here:
https://www.sdiarticle5.com/review-history/106326